7-1-2006

Adsorption of transition-metal atoms on boron nitride nanotube: A density-functional study

Xiaojun Wu
University of Nebraska-Lincoln, jwu4@unl.edu

Xiao Cheng Zeng
University of Nebraska-Lincoln, xzeng1@unl.edu

Adsorption of transition-metal atoms on boron nitride nanotube: A density-functional study

Xiaojun Wu and X. C. Zeng[a)]
Department of Chemistry, University of Nebraska-Lincoln, Lincoln, Nebraska 68588 and Nebraska Center for Materials and Nanoscience, University of Nebraska-Lincoln, Lincoln, Nebraska 68588

(Received 3 April 2006; accepted 5 June 2006; published online 27 July 2006)

Adsorption of transition atoms on a (8,0) zigzag single-walled boron nitride (BN) nanotube has been investigated using density-functional theory methods. Main focuses have been placed on configurations corresponding to the located minima of the adsorbates, the corresponding binding energies, and the modified electronic properties of the BN nanotubes due to the adsorbates. We have systemically studied a series of metal adsorbates including all 3*d* transition-metal elements (Sc, Ti, V, Cr, Mn, Fe, Co, Ni, Cu, and Zn) and two group-VIIIA transition-metal elements (Pd and Pt). We found that many transition-metal atoms can be chemically adsorbed on the outer surface of the BN nanotubes and that the adsorption process is typically exothermic. Upon adsorption, the binding energies of the Sc, Ti, Ni, Pd, and Pt atoms are relatively high (>1.0 eV), while those of V, Fe, and Co atoms are modest, ranging from 0.62 to 0.92 eV. Mn atom forms a weak bond with the BN nanotube, while Zn atom cannot be chemically adsorbed on the BN nanotube. In most cases, the adsorption of transition-metal atoms can induce certain impurity states within the band gap of the pristine BN nanotube, thereby reducing the band gap. Most metal-adsorbed BN nanotubes exhibit nonzero magnetic moments, contributed largely by the transition-metal atoms. © *2006 American Institute of Physics*. [DOI: 10.1063/1.2218841]

INTRODUCTION

Since the discovery of carbon nanotubes,[1] tubular nanomaterials have attracted considerable attention due to their unique physical, chemical, and mechanical properties as well as their great potential for applications. A fundamental example relevant to the physical and chemical properties of nanotubes is the interaction between nanotubes and metal atoms. A better understanding of the metal/nanotube interaction will have potential impacts on applications such as catalysis, sensors, fabrication of core/sheath nanostructures, and nanoelectronics. Furthermore, a better understanding of the interaction between magnetic atoms and nanotubes can be of importance to the field of low-dimensional magnetic systems. Thus far, most previous experimental and theoretical studies of metal/nanotube interactions have been mainly devoted to the carbon nanotube/transition-metal systems. The metal component can be a single atom, a metal cluster, or a planar metal surface.[2–4] Many previous studies have provided fundamental insights into potential applications of metal-adsorbed carbon nanotubes in various fields. The fact that the electronic properties of carbon nanotubes can be either metallic or semiconducting, depending on the tube diameter and helicity,[5] also renders metal-adsorbed carbon nanotubes a versatile tubular nanomaterials. On the other hand, because of the dependence of the electronic properties on the helicity and diameter, a separation process must be incurred to collect carbon nanotubes with uniform electronic properties. This separation process poses a hindrance to future massive application of carbon nanotubes in nanoelectronics.

Boron nitride (BN) nanotubes, another prevailing tubular nanomaterial which was successfully synthesized shortly after the discovery of the carbon nanotubes, are known to be wide-gap semiconductors whose band gaps ($\sim$5.5 eV) are almost independent of the tube diameter, helicity, and the number of walls. During the growth process, BN nanotubes tend to select a nonhelical or zigzag orientation. Like carbon nanotubes, BN nanotubes also possess many unique physical and mechanical properties such as strong hardness, high thermal stability, and chemical inertness,[6–9] which have promoted increasing number of studies of this tubular nanomaterial. To date, fewer research work have been reported on the BN nanotube/metal systems, compared to the amount of work reported on the carbon nanotube/metal systems. One known feature about the interaction between a BN nanostructure and metal is that the graphitelike BN surface is much more difficult to wet by metals than the carbon graphite surface. Recently, several experimental efforts have been made to fill the BN nanotubes with 3*d* transition metals, such as Fe–Ni Invar alloy, Co, Mo, Ni, and $NiSi_2$.[10–14] On the theoretical side, several studies on the filling the BN nanotubes with transition metals have been reported, wherein half-metallic behavior has been seen in some of these systems.[15,16]

In this paper, we report a systematic study of the interaction between the BN nanotube and all 3*d* transition metals and two group-VIIIA metals using spin-polarized density-functional theory (DFT). For all DFT calculations, the indi-

[a)]Electronic mail: xczeng@phase2.unl.edu

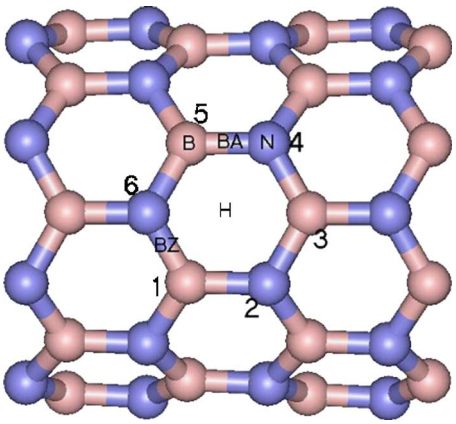

FIG. 1. (Color online) The optimized structure of a pristine (8,0) zigzag single-walled BN nanotube.

vidual metal atom is placed on the outer surface of a (8,0) zigzag single-walled BN nanotube. Configurations corresponding to the local minima (including the most stable configuration) of the metal atoms on the BN nanotubes, the corresponding binding energies, and the modified electronic structures of BN nanotubes due to metal adsorption are calculated. We found that the binding energies can vary significantly with different metal atoms, but change little at different adsorption sites for a given metal. The adsorption of one metal atom per supercell can induce impurity states within the band gap of the pristine BN nanotube, thereby causing the band gap reduction. With different transition metals, the BN nanotube can exhibit a magnetic moment ranging from 0 (for Ni) to $5.0\mu_B$ (for Mn). Our calculations show that some metal atoms can strongly bind to the BN nanotube. Thus, the BN nanotube may be covered (or wet) by metal atoms, which may lead to potential applications in future molecular electronics.

MODELS AND METHODS

The DFT calculations were carried out using linear combination of atomic orbitals density-functional method implemented in the DMOL3 package.[17] All-electron calculations were performed with the double numerical basis sets plus polarization functional (DNP) and the generalized-gradient approximation (GGA) with the Perdew-Burke-Ernzerhof (PBE) functional.[18] The DNP basis sets are comparable to 6-31G** Gaussian basis sets.[19] Delley *et al.* showed that the DNP basis sets are more accurate than the Gaussian basis sets of the same size.[17] For the 5*d* transition metals Pd and Pt, scalar relativistic effect is taken into account when dealing with their core electrons. The real-space global cutoff radius was set to be 5.5 Å. Spin-unrestricted DFT was used to obtain all the results presented in this work. Without losing generality, we chose the (8,0) zigzag single-walled BN nanotube as a prototype model system since the electronic properties of BN nanotubes are weakly dependent on the tube diameter and helicity. A tetragonal supercell is used, whose size is $20\times20\times8.64$ Å^3, with the length of c (in the axial or z direction) being twice of the periodicity of the (8, 0) BN nanotube. The supercell contains 32 B and 32 N atoms as well as a single metal atom. With the periodic conditions,

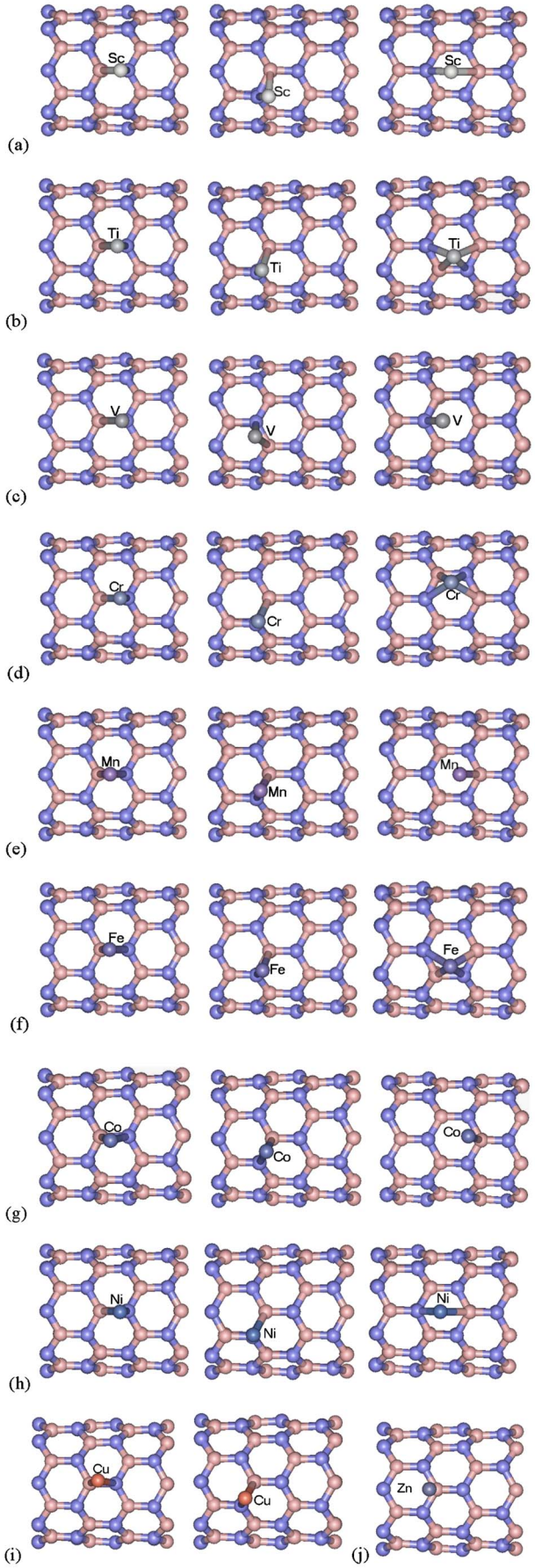

FIG. 2. (Color online) Local minima configurations of the 3*d* transition-metal atom [(a)–(j)] adsorbed on the outer surface of the (8,0) BN nanotube.

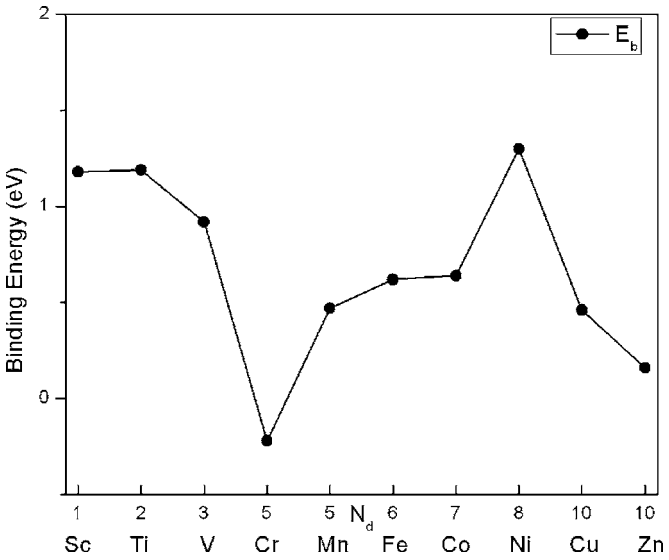

FIG. 3. The binding energies E_b (at the most stable configuration of metal atoms) vs the number of d electrons N_d of the first-row transition metals.

the nearest distance between two BN nanotubes is no less than 14.0 Å. The Brillouin zone is sampled by $1\times1\times3$ special k point using the Monkhorst-Pack scheme.[20] Test calculation showed that results are not changed upon increasing the k points.

RESULTS AND DISCUSSION

Ten 3d transition metals (Sc, Ti, V, Cr, Mn, Fe, Co, Ni, Cu, and Zn) and two group-VIIIA transition metals (Pd and Pt) have been considered to be the adsorbate on the outer surface of the (8,0) BN nanotube. For each type of the adsorbate, five different initial adsorption sites were selected to examine the nanotube/metal interaction. The five sites are (1) the top site of the boron atom (B), (2) the top site of the nitrogen atom (N), (3) the hollow site of the B_3N_3 hexagon ring (H), (4) the bridge site over an axial BN bond (BA), and (5) the bridge site over a zigzag BN bond (BZ), all shown in Fig. 1. To ensure that the most stable adsorption configuration can be achieved, the initial distance between the metal atom and the sidewall surface was adjusted several times from 1.5 to 3.0 Å. Full structural relaxation was then performed with each initial metal-tube distance.

In Figs. 2(a)–(j), configurations corresponding to the local minima are displayed for each of the ten 3d transition metals adsorbed on the BN nanotube (BNNT). The binding energies for all stable configurations are summarized in Table I. Here, the binding energies are given by the equation

$$E_b = E_T(\mathrm{BNNT}) + E_T(A) - E_T(\mathrm{BNNT}+A), \quad (1)$$

where E_T(BNNT) denotes the spin-polarized total energy (per supercell) for the pristine BN nanotube, $E_T(A)$ is the energy of a single atom A, and E_T(BNNT+A) is the total energy of the BN nanotube with the adsorbed A atom (per supercell).

Using the Sc case as an example [Fig. 2(a)], for which three stable configurations at the BA, BZ, and H sites are obtained, whereas the adsorption at the B and N sites is unstable. Upon structural relaxation at the B and N sites, the Sc atom will spontaneously relocate to take one of the three stable configurations. At the BA site, the B–Sc and N–Sc bond lengths are 2.31 and 2.15 Å, respectively. At the BZ site, the two bond lengths are 2.24 and 2.16 Å, close to those at the BA site. At the H site, the Sc atom locates right above the center of the B_3N_3 hexagonal ring at the height of ~1.8 Å. The three B–Sc bonds lengths are 2.30, 2.72, and 2.73 Å, and three N–Sc bonds lengths are 2.27, 2.69, and 2.67 Å, respectively. The results show that the Sc atom tends to locate closer to the three N atoms than B atoms. The calculated binding energies range from 1.06 to 1.18 eV for the three stable configurations. The positive binding-energy value indicates that the chemical adsorption process is exothermic. Note also that the binding energies as well as the B–Sc and N–Sc bond lengths change little at the three adsorption sites.

Among other nine transition-metal elements considered, the Ti, V, Cr, Mn, Fe, Co, and Ni atoms can be chemically adsorbed on the BA, BZ, and H sites as well, whereas the adsorption on the B or N site is unstable. The B–M (M =Ti, V, Cr, Mn, Fe, Co, and Ni) bond lengths range from 2.05 to 2.52 Å while the N–M bond lengths range from 1.85 to 2.40 Å. In contrast, at the H site, six of the seven metal atoms can no longer locate above the center of the B_3N_3 hexagonal ring but either near the B–N bond that is parallel to the tube axis (for Ti, Cr, and Fe), or near the B atom (for Mn and Co) or the N atom (for V); only the Ni atom can locate right above the center of the B_3N_3 hexagonal ring at the height of 1.6 Å. More different from the Sc case, Cu atom can only be chemically adsorbed at the BA and BZ sites, while Zn atom can only be physically adsorbed above the B site at a height of ~3.7 Å. Again, as in the case Sc adsorption, the calculated binding energies as well as the B–M and N–M bond lengths change little at different adsorption sites for nearly all the 3d transition metals.

In Fig. 3, we plot the binding energies corresponding to the most stable configurations E_b versus the number of d electrons N_d of the ten 3d transition-metal elements. Interestingly, the trend in the variation of E_b vs N_d is mostly similar to that in the cases of adsorption of the 3d transition-metal atoms on the carbon nanotubes, while the values of the binding energies are slightly smaller than those of 3d transition-metal atoms adsorbed carbon nanotubes.[2] Here, there are two maxima in the E_b vs N_d curve, one at N_d=2 and the other at N_d=8, and the curve shows a minimum at N_d=5 (Cr). The binding energy of Ni (N_d=8) is the highest among the ten 3d transition-metal elements. As shown in Fig. 3, some atoms such as Sc, Ti, and Ni can bind strongly with the BN nanotube (with the binding energies >1.0 eV), and some others such as V, Fe, and Co can still be chemically adsorbed on the sidewall but with modest binding energies (ranging from 0.62 to 0.92 eV). The binding between Mn or Cu atom and the BN nanotube is only marginal with the binding energy <0.50 eV. Two unusual cases are Zn and Cr. The former metal atom cannot be chemically adsorbed on the BN nanotube, for which the binding mainly stems from the van de Waals interaction. For Cr, although a stable adsorption configuration on the BN nanotube can be achieved, the calculated binding energy suggests that the adsorption process is

TABLE I. Calculated binding energies (E_b) of a single metal atom (per supercell) adsorbed on the (8,0) BN nanotube at three stable binding sites, the corresponding boron-metal, nitrogen-metal bond distances, and boron-metal-nitrogen angle, the net magnetic moment of the metal atom/total system, and the charge transferred (C) from the metal atom to BN nanotube. (M denotes the metal atom and B and N atoms are labeled in Fig. 1.)

Atom	Site	$\text{Bond}_{\text{B}-M}$ (Å)	$\text{Bond}_{\text{N}-M}$ (Å)	$\angle_{\text{B}-M-\text{N}}$ (°)	E_b (eV)	$\mu_{\text{M}}/\mu_{\text{total}}$ (μ_B)	C (e)
Sc	BA	2.31	2.15	40.3	1.08	0.88/1.0	0.35
	BZ	2.24	2.16	43.9	1.06	0.90/1.0	0.35
	H	2.30,[a],2.72,[b]2.73[c]	2.27,[d]2.69,[e]2.67[f]	77.4[g]	1.18	0.94/1.0	0.32
Ti	BA	2.50	2.35	42.6	1.18	3.39/4.0	0.12
	BZ	2.22	2.15	35.2	1.19	1.96/2.0	0.28
	H	2.25,2.44,2.98	2.34,2.34,2.93	76.0	1.19	1.87/2.0	0.30
V	BA	2.52	2.19	35.7	0.85	4.39/5.0	0.08
	BZ	2.51	2.19	36.5	0.92	4.34/5.0	0.08
	H	2.90,2.74,2.74	2.22,2.98,2.98	66.5	0.79	4.29/5.0	0.05
Cr	BA	2.19	2.04	42.1	−0.22	4.08/4.0	0.32
	BZ	2.18	2.03	44.5	−0.23	4.05/4.0	0.32
	H	2.20,2.95,2.08	2.20,2.95,2.07	79.8	−1.17	2.12/2.0	0.39
Mn	BA	2.19	2.31	38.8	0.47	4.99/5.0	0.20
	BZ	2.19	2.34	39.7	0.46	4.99/5.0	0.19
	H	2.21,2.98,2.98	2.74,2.72,2.72	69.4	0.42	4.98/5.0	0.21
Fe	BA	2.17	2.37	37.8	0.62	3.87/4.0	0.10
	BZ	2.23	2.29	39.2	0.62	3.86/4.0	0.10
	H	2.12,2.01,2.88	2.15,1.97,2.87	82.1	−0.27	2.20/2.0	0.22
Co	BA	2.15	2.30	38.7	0.64	2.90/3.0	0.08
	BZ	2.16	2.40	38.3	0.62	2.81/3.0	0.09
	H	2.14,3.19,3.02	3.03,2.78,2.57	64.7	0.65	2.79/3.0	0.10
Ni	BA	2.05	1.85	44.9	1.30	0.00/0.0	0.11
	BZ	2.10	1.85	45.2	1.27	0.00/0.0	0.11
	H	2.21,2.40,2.41	1.98,2.50,2.51	83.8	0.81	0.00/0.0	0.09
Cu	BA	2.33	2.27	36.8	0.46	0.78/1.0	0.06
	BZ	2.27	2.36	37.7	0.44	0.76/1.0	0.10
	H	→ BA					
Zn		~3.7	~4.0		0.16	0.00/0.0	
Pd	BA	2.21	2.14	39.9	1.33	0.00/0.0	0.22
	BZ	2.28	2.13	40.4	1.32	0.00/0.0	0.22
	H	→ BA					
Pt	BA	2.19	1.98	42.4	1.80	0.00/0.0	0.12
	BZ	2.43	1.96	38.7	1.71	0.00/0.0	0.11
	H	→ BA					

[a]B1−M.
[b]B3−M.
[c]B5−M.
[d]N2−M.
[e]N4−M.
[f]N6−M.
[g]∠B3−M−N6.

endothermic. In summary, based on the calculated binding energies, we speculate that those metals that can bind strongly with the BN nanotube might form a uniform coverage on the tube sidewall, while those cannot are more likely to form clusters on the sidewall as the number of the metal atoms grows.

In addition to the binding energies and local-minimum configurations, we have also examined possible modification of the electronic structures of the BN nanotube by the chemical adsorption of 3d transition-metal atoms. Based on the spin unrestricted calculation, the band structures of the pristine (8,0) BN nanotube as well as those of the nine BNNT/metal systems (except BNNT/Zn) with the metal atom at the BA, BZ, and H sites are calculated. Both the plus and minus spins (labeled with "+" and "−" in Fig. 4) were considered. For the pristine BN nanotube, the band structures for the plus

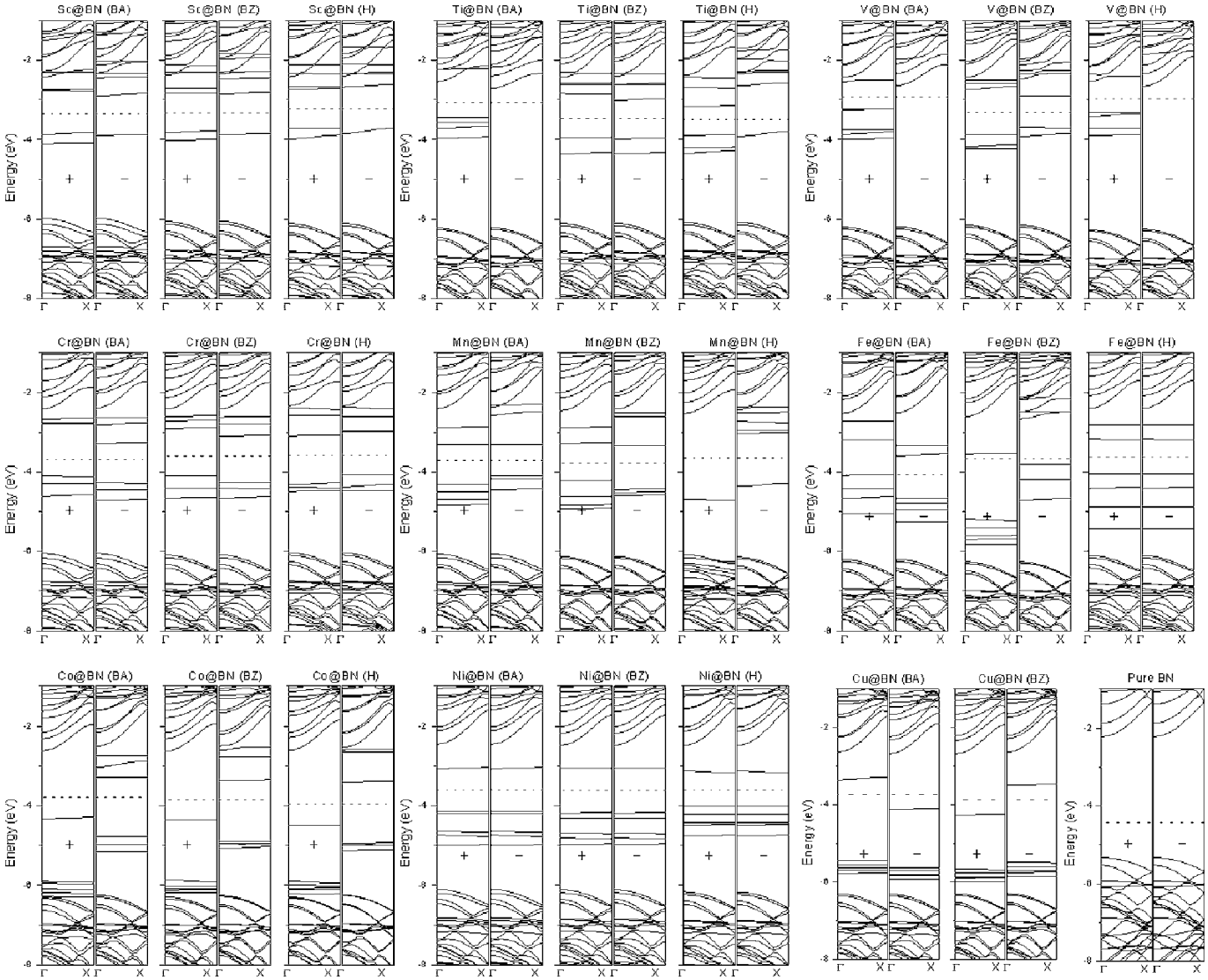

FIG. 4. The band structures of metal-adsorbed BN nanotube. The plus and minus spin electronic structures are distinguished with "+" and "−." The Fermi level is plotted with the dotted line. The Γ and *X* represents two highly symmetric points in the Brillouin zone of the supercell, that is, (0, 0, 0) and (0, 0, 0.5), respectively.

and minus spins are the same, showing a direct band gap of 3.65 eV that is nearly the same as previous results.[5,6] As shown in Fig. 4, it can be seen that in all nine systems the chemical adsorption of the 3*d* transition-metal atoms induces certain impurity states within the band gap of the pristine BN nanotube, thereby causing the band gap reduction. In most cases, the band gap is no greater than 1.0 eV. The results of projected density of states (PDOS) show that these impurity states are mainly due to the *d* and *s* electrons of the transition metals. To some extent, the *p* electrons also contribute to the density of states near the Fermi level, but the contribution is much less than that from the *d* and *s* electrons. The BN nanotube contributes little to the density of states near the Fermi level. It is worthy to note that when Fe atoms are adsorbed at the BA site, the calculated band structures suggest that this particular BNNT/Fe configuration is possibly a half-metal. A band crossing at the Fermi level occurs with little dispersion in the plus-spin band structures, due mainly to the *s* electrons of the Fe atoms. In the minus-spin band structures, however, there is a band gap of ~1.0 eV. Again, the band structures of BNNT/*M* (*M*=Sc, Cr, Co, and Ni) change little with different adsorption sites.

The electron-charge analysis using the Hirshfeld method is summarized in Table I. Note that the Hirshfeld charge analysis is based on the deformation electron density, which seems less sensitive to the selected basis sets than the Mulliken charge analysis, although the Hirshfeld charge analysis generally underestimates the atomic charges.[21] With the 3*d* transition-metal atoms adsorbed on the sidewall of BN nanotube, the Hirshfeld analysis indicates that certain amount of charge is transferred from the metal atoms to the BN nanotubes. As a result, a net magnetic moment may emerge, ranging from $5.0\mu_B$ (for Mn) to 0 (for Ni). The net spin mainly locates on the metal atoms. Understandably, because the ground state of the pristine BN nanotube is nonmagnetic, the net spin should origin from the magnetism of the adsorbed metal atoms. Note also that in the case of transition-metal atoms adsorbed on the graphite or carbon nanotubes, previ-

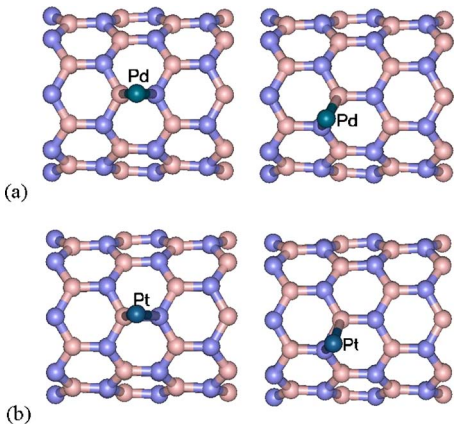

FIG. 5. (Color online) Local minima configurations of a (a) Pd and (b) Pt atom (in the supercell) adsorbed on the (8,0) BN nanotube.

ous studies have shown distinct deduction of the local magnetic moment on the transition-metal atoms due to the promotion of the 4*s* electrons into 3*d* orbitals.[2,3,22] However, in the case of transition-metal atoms adsorbed on the BN nanotubes, the deduction of the magnetic moment is not as much. Consequently, the local magnetic moments of many transition-metal atoms are close to those of freestanding transition-metal atoms. Moreover, the net spin depends only weakly on the location of the adsorption site for many transition metals, a unique feature that could be exploited for making molecular magnets with the metal-covered BN nanotubes. Three exceptions are Ti, Cr, and Fe, for which the magnetic moment can vary with the location of the adsorption site. One possible reason for the exceptions is that the obtained adsorption configuration is only a local minimum with different magnetic moments. Interestingly, this variation of the magnetic moment seems also correlate with the charge transfer from the metal atoms to the BN nanotube (see the last two columns of Table I).

Lastly, the interaction between two group-VIIIA transition-metal element, Pd and Pt, and the BN nanotube is studied because these two metals are popular catalysts. Local-minimum configurations of the Pt and Pd atom on the BN nanotube are shown in Figs. 5(a) and 5(b). Both metal atoms can be chemically adsorbed at the BA and BZ sites, but the adsorption at the H, B, and N sites is unstable. The B–*M* and N–*M* (*M*=Pd and Pt) bond lengths range from 1.96 to 2.43 Å, nearly independent of the adsorption site. The calculated binding energies are 1.33 and 1.23 eV for Pd at the BA and BZ sites, and 1.80 and 1.71 eV for Pt at the BA and BZ sites, respectively. Like in the case of first-row transition-metal adsorption, the adsorption of Pd or Pt atoms can induce six impurity states within the band gap of the BN tube (Fig. 6). One of the six impurity states is unoccupied, while the other five are occupied. As such, the band gap of the BNNT/*M* systems (*M*=Pd and Pt) is about 2.10 eV. The PDOS analysis indicates that the unoccupied state origins mainly from the *s* electrons of the metal atoms and the occupied states mainly origin from the *d* electrons of the metal atoms. Moreover, both the BNNT/Pd and BNNT/Pt systems exhibit zero magnetism moment.

CONCLUSION

Using the density-functional theory, the adsorption of transition-metal atoms on the (8,0) zigzag single-walled BN nanotube has been systemically studied. Ten 3*d* transition metals (from Sc to Zn) and two group-VIIIA elements, Pd and Pt, were considered. We found that most transition metals can be chemically adsorbed on the sidewall of BN nanotube and the adsorption process is typically exothermic. Several metal atoms such as Sc, Ti, Ni, Pd, and Pt can be chemically adsorbed with relatively high binding energy (greater than 1.0 eV). The Mn atom can only form a weak chemical bond with the BN nanotube while Zn atoms cannot be chemically adsorbed on the BN nanotube at all. In most cases, the binding energies are less sensitive to the adsorption sites. On the electronic structures, the adsorption of metal atoms generally induces some impurity states within the band gap of the pristine BN tube. These impurity states are mainly due to the *s* and *d* electrons of the metal atoms. The transition-metal adsorbed BN nanotubes are all semiconductors with reduced band gaps except the Fe-adsorbed BN nanotube (on the BA site) which may result in a half-metal.

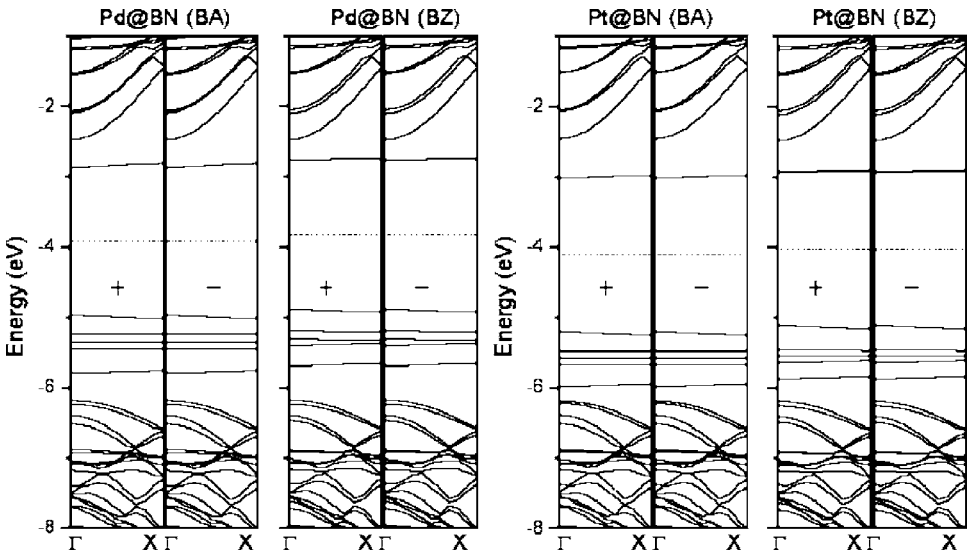

FIG. 6. The band structures of the Pd- and Pt-adsorbed (8,0) BN nanotubes. The Fermi level is plotted with the dotted line. The plus and minus spin band structures are distinguished with + and −.

Finally, the adsorption of the transition-metal atoms can give rise to a variety of net magnetic moments, ranging from $5.0\mu_B$ to 0.

ACKNOWLEDGMENTS

We are grateful to valuable discussions with Professor J. L. Yang. This work is supported by grants from the DOE (DE-FG02-04ER46164), the Nebraska Research Initiative, and by John Simon Guggenheim Foundation and the Research Computing Facility at University of Nebraska-Lincoln.

[1] S. Iijima, Nature (London) **354**, 56 (1991).
[2] E. Durgun, S. Dag, V. M. K. Bagci, O. Gülseren, T. Yildirim, and S. Ciraci, Phys. Rev. B **67**, 201401 (2003).
[3] Y. Yagi, T. M. Briere, M. H. F. Sluiter, V. Kumar, A. A. Farajian, and Y. Kawazoe, Phys. Rev. B **69**, 75414 (2004).
[4] C.-K. Yang, J. J. Zhao, and J. P. Lu, Phys. Rev. B **66**, 41403 (2002).
[5] R. Saito, M. Fujita, G. Dresselhaus, and M. S. Dresselhaus, Phys. Rev. B **46**, 1804 (1992).
[6] A. Rubio, J. L. Corkill, and M. L. Cohen, Phys. Rev. B **49**, 5081 (1994).
[7] E. Bengu and L. D. Marks, Phys. Rev. Lett. **86**, 2385 (2001).
[8] H. J. Xiang, J. L. Yang, J. G. Hou, and Q. S. Zhu, Phys. Rev. B **68**, 035427 (2003).
[9] A. Loiseau, F. Willaime, N. Demoncy, G. Hug, and H. Pascard, Phys. Rev. Lett. **76**, 4737 (1996).
[10] Y. B. Li, P. S. Dorozhkin, Y. Bando, and D. Golberg, Adv. Mater. (Weinheim, Ger.) **17**, 545 (2005).
[11] W. Q. Han, P. Redlich, F. Ernst, and M. Rühle, Appl. Phys. Lett. **75**, 1875 (1999).
[12] R. Z. Ma, Y. Bando, and T. Sato, Chem. Phys. Lett. **350**, 1 (2001).
[13] C. C. Tang, Y. Bando, D. Golberg, X. X. Ding, and S. R. Qi, J. Phys. Chem. B **107**, 6539 (2003).
[14] D. Golberg, F. F. Xu, and Y. Bando, Appl. Phys. A: Mater. Sci. Process. **76**, 479 (2003).
[15] H. J. Xiang, J. L. Yang, J. G. Hou, and Q. S. Zhu, New J. Phys. **7**, 39 (2005).
[16] Z. Zhou, J. J. Zhao, Z. F. Chen, X. P. Gao, J. P. Lu, P. v. R. Schelyer, and C.-K. Yang, J. Phys. Chem. B **110**, 2529 (2006).
[17] B. Delley, J. Chem. Phys. **92**, 508 (1990); Int. J. Quantum Chem. **69**, 423 (1998); J. Chem. Phys. **113**, 7756 (2000); Phys. Rev. B **65**, 085403 (2002); A. Kessi and B. Delley, Int. J. Quantum Chem. **68**, 135 (1998).
[18] J. P. Perdew, K. Burke, and M. Ernzerhof, Phys. Rev. Lett. **77**, 3865 (1996); **78**, 1396(E) (1997).
[19] W. J. Hehre, L. Radom, P. v. R. Schlyer, and J. A. Pople, *Ab Initio Molecular Orbital Theory* (Wiley, New York, 1986).
[20] H. J. Monkhorst and J. D. Pack, Phys. Rev. B **13**, 5188 (1976).
[21] F. L. Hirshfeld, Theor. Chim. Acta **44**, 129 (1977).
[22] D. M. Duffy and J. A. Blackman, Phys. Rev. B **58**, 7443 (1998).